

## NUMERICAL ANALYSIS FOR THE DYNAMIC RESPONSE CHARACTERISTICS OF THE PRESTRESSED CONCRETE SLEEPER

Tsutomu Watanabe<sup>1</sup>, Kodai Matsuoka<sup>1</sup>, and Shintaro Minoura<sup>1</sup>

<sup>1</sup> Railway Technical Research Institute  
address 2-8-38 Hikari-cho Kokubunji-shi Tokyo Japan  
e-mail: watanabe.tsutomu.30@rtri.or.jp

**Keywords:** Prestressed concrete sleeper, Railway track, Rail joint, Impact load, Numerical analysis, Dynamic interaction.

**Abstract.** *The Prestressed concrete sleeper (PC sleeper) has many advantages over the wooden sleeper in terms of maintenance, load bending capacity, weight and lateral ballast resistance force. In Japan, the PC sleeper has been widely used since 1951. The PC sleeper is designed in consideration of the impact wheel load which is mainly caused by a rail joint or wheel flat. This research focused on the impact wheel load at rail joints. By field measurements in an operating line and numerical analyses, the dynamic response characteristic of the PC sleeper was clarified. The field measurement of PC sleeper behavior shows that the maximum bending moment of a PC sleeper with a rail joint during train running is almost 4 times larger than that in plain sections, and the maximum bending moment of the PC sleeper adjacent to the rail joint is almost 2.7 times larger than that in plain sections. The numerical analysis shows that support condition has the greatest influence on the bending moment of the PC sleeper among various parameters. Furthermore, the impact wheel load caused by a rail joint affects dynamic behavior of PC sleepers within 4m from the rail joint.*

## 1 INTRODUCTION

A prestressed concrete sleeper (PC sleeper) is designed mainly in consideration of an impact wheel load during the train running. The impact load is generally caused by the wheel flat, the rail joint, the welded joint irregularity of the rail and the railhead corrugation. Among those defects, the wheel flat and the rail joint have the greatest influence on the dynamic response of the PC sleeper. At the beginning of the development of the PC sleeper, it had been thought that the enormous impact wheel load was mainly induced by the wheel flat [1, 2]. For this reason, a large number of researches into the wheel flat have been conducted [3, 4]. Through the running test and the impact load examination of the PC sleepers, these researches made clear that the design load of the PC sleeper shall be the 4 times larger than the static load in order to allow no tensile stress (full prestressing) under the assumed maximum impact load by wheel flat. Such knowledge and information have been used for the design of PC sleepers in Japan [1]. Recently, various kinds of research and development have been promoted from the viewpoint of the optimization of the sleeper [5-10].

On the other hand, particularly in Japan, though the rail joint has been recognized as another serious source of the impact wheel load, the research into the effect of the impact wheel load generated by the rail joint has been insufficient. This is due to the fact that the suspended rail joint, that is, the rail joint installed between adjacent two sleepers has been widely introduced in an attempt to prevent the impact wheel load as a standard installation method of the rail with wooden or PC sleepers. For example, though the PC sleepers that are adjacent to the rail joint are affected by the impact wheel load caused by the rail joint, the longitudinal span of the influence of the impact wheel load and the effect of the rail joint irregularity have not been sufficiently investigated. Recently, in Japan, a specified type of PC sleeper which is installed directly under the rail joint has been increasingly used. Thus, the phenomenon elucidation of the dynamic response of the PC sleepers at or adjacent to the rail joint is required. Furthermore, the most suitable design of the PC sleeper according to the track condition is also being required [11].

The dynamic response of the PC sleeper at rail joints includes a high frequency phenomenon within 1/1000 seconds. Recently, tools for the phenomenon elucidation of the dynamic response of the PC sleeper at rail joints are gradually being provided such as high quality measurement systems (high frequency and multi-channel synchronized measurement) of the spread of high spec. supercomputers.

Against these backgrounds, this research focused on the impact wheel load at rail joints paying attention to the following points.

- (1) Conduct the field measurement in an operating line in order to elucidate the bending moment of the PC sleeper during the train running at rail joints and in plain track sections.
- (2) Develop three dimensional numerical analysis models by a finite element method.
- (3) Evaluate the effect of the various parameters of the vehicle or track on the bending moment of the PC sleeper quantitatively.
- (4) Evaluate the longitudinal span of the influence of the impact wheel load at rail joints.

## 2 INVESTIGATION METHOD

### 2.1 Field measurement method

Figure 1 shows the outline of the track. In this section, standard rails of 25m in length and 60kg/m in weight are used and there are rail joints at an interval of 25m. PC sleepers are type-6 PC sleepers in the plain section and PC sleepers at the rail joints are those standardized in Japanese Industrial Standard (JIS). The numbers of PC sleepers per rail (25m in length) is 41.

The field measurement of the bending moment of PC sleepers during the train passing was conducted on two rail joint PC sleepers (Joint 1, Joint 2), two type-6 PC sleepers adjacent to the rail joint (A and B) and two type-6 PC sleepers (C and D). The type-6 PC sleepers C and D are in the plain section. Trains running in this section are Japanese standard commuter trains with the static nominal wheel load of almost 50kN.

Figure 2 shows the positions of strain gauge on the PC sleeper. In total, four strain gauges per sleeper were used, two of which were attached on the side of the PC sleeper (one at an upper position and the other at a lower position) at its longitudinal center and the other two strain gauges were attached in the same manner at its rail seat position. Strain gauges made in KYOWA ELECTRONIC INSTRUMENTS CO. were used for the field measurement, and a built-in chassis made in NATIONAL INSTRUMENTS CO. were used to acquire the experimental signals from 32-channel strain gauge units. The sampling rate is 5000Hz.

Figure 3 shows the measurement method of the vibration mode of the PC sleeper. Seven piezoelectric accelerometers were installed on the top of the PC sleeper. The piezoelectric accelerometers were made in RION CO. (PV-85). Measured response of the accelerometer was recorded in a laptop PC with 5000Hz sampling via preamplifier and A/D converter. Vibration characteristics were identified by the ERA (Eigensystem Realization Algorithm) method [12, 13], which can identify the character matrix of linear time-invariant systems with the principles of minimal realization. The MAC (Modal Amplitude Coherence) value on the controllability was applied to the accuracy evaluation of the vibration characteristics. 40 degrees of freedom were set in order to identify the major modes of the PC sleeper. When the MAC value is 0.99 or more, it is judged to be the vibration mode characteristic of the PC sleeper.

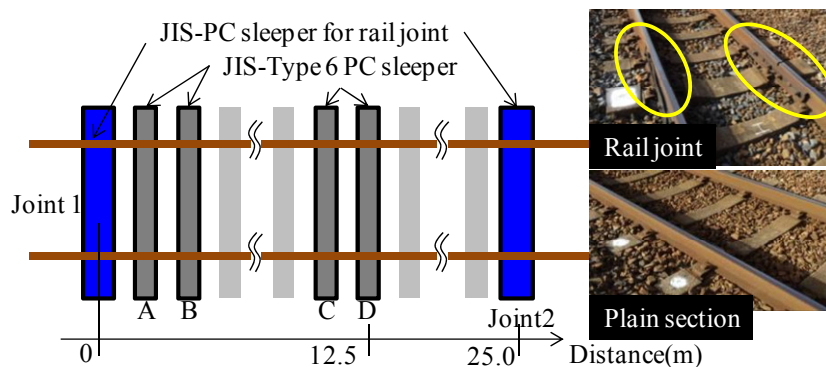


Figure 1: Outline of the track.

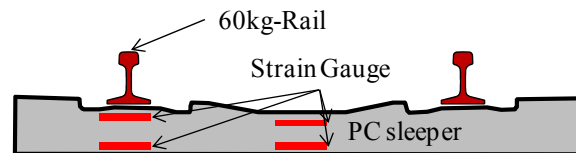


Figure 2: Positions at which to attach the strain gauges to the PC sleeper.

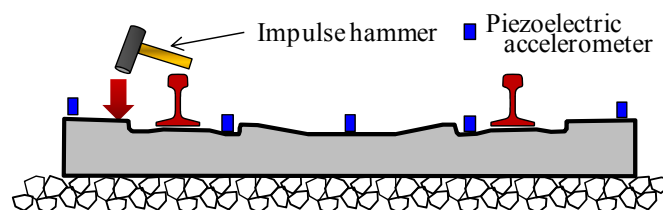


Figure 3: Measurement method of the vibration mode of the PC sleeper on the impulse hammer test.

## 2.2 Numerical analysis method

### (1) Dynamic model of the track

Figure 4 shows the outline of the three dimensional numerical analysis model of the target track. The DIASTARSIII program developed by the Railway Technical Research Institute was used for numerical analysis [14, 15].

The track was modeled using the finite element method. Assembling all elements in the total model, the equation of motion of the track is obtained in a standard matrix form as

$$M^B \ddot{X}^B + C^B \dot{X}^B + K^B X^B = F_L^B + F_F^B(X^V, X^B) + F_N^B(X^B) \quad (1)$$

where  $X^B$  is the displacement vector of the track, and  $M^B$ ,  $C^B$  and  $K^B$  are the mass, damping and stiffness matrices, respectively;  $F_L^B$  is load vectors;  $F_F^B(X^V, X^B)$  is the interaction force between the rail and the car,  $F_N^B(X^B)$  is the load vectors of non-linear spring force in the track.

As shown in Figure 4, the rail and sleepers were modeled using beam elements, and the rail pads, the ballast and the roadbed were modeled using spring elements. The basic rail mesh size was set at 35mm and the PC sleeper mesh size was set at 55mm. The total number of nodal points is 8338 and the total numbers of elements is 13012.

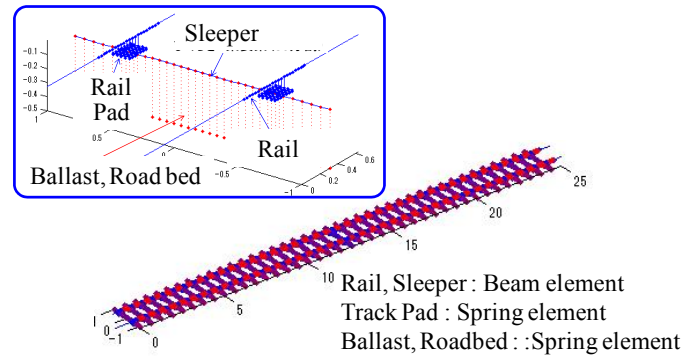


Figure 4: Outline of the three dimensional numerical analysis model of the target track.

### (2) Dynamic model of the vehicle

Figure 5 shows the dynamic model of the vehicle assuming that a body, bogies and wheelsets are rigid. These three-dimensional rigid elements are linked by springs  $K_N$  and dampers  $C_N$  ( $N$  is a suffix in Figure 5) according to their respective characteristics. The train has 31 degrees of freedom (5 degrees of freedom for the body, 5 degrees of freedom for the bogies, and 4 degrees of freedom for the wheelset) per one car. The train consists of multiple vehicle models linked together by springs  $K_C$  and dampers  $C_C$  attached to the ends of the vehicle models. Assuming that the train runs at a constant speed, the equation of three dimensional motion of the train with  $N$  vehicles is written in a matrix form as shown in reference [16].

$$M^V \ddot{X}^V + C^V \dot{X}^V + K^V X^V = F_L^V + F_F^V(X^V, X^B) + F_N^V(X^V) \quad (2)$$

where, superscript V and B are the vehicle and the track, respectively;  $X^V$  is the displacement vector of the vehicle;  $M^V$ ,  $C^V$  and  $K^V$  are the mass, damping and stiffness matrices of the vehicle, respectively;  $F_L^V$  is load vectors;  $F_F^V(X^V, X^B)$  is the interaction force between the rail and the vehicle,  $F_N^V(X^V)$  is the load vectors of non-linear spring force in the car. In this research, the train consists of six Japanese standard commuter vehicles with a length of 20 m and an axle load of almost 50 kN.

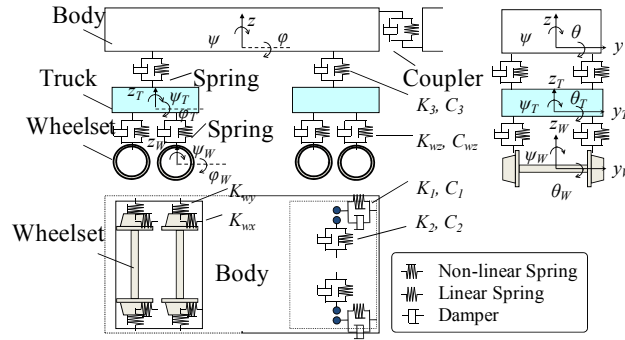


Figure 5: Dynamic model of vehicle.

### (3) Dynamic model of the interaction force between the wheel and the rail

Figure 6 shows the wheel/rail model. We focused on relative displacement between the wheel and the rail. The vertical interaction force between these components was modeled by *Hertzian* contact springs so that it is possible to judge the contact condition between the wheel and rail. The vertical relative displacement between the rail and the wheel  $\delta_z$  is expressed by equation (3).

$$\delta_z = z_R - z_W + e_z + e_{z0}(y) \quad (3)$$

where  $z_R$  is the rail vertical displacement,  $z_W$  is the wheel vertical displacement,  $e_z$  is the vertical track irregularity.  $e_{z0}(y)$  is the wheel radius variation in the current wheel contact point. When  $\delta_z \geq 0$ , the wheel is in contact with the rail, and  $\delta_z \leq 0$ , the wheel is loss of contact with the rail. The z-direction interaction force  $H$  produced due to the contact of the wheel and the rail is expressed by equation (4).

$$H = H(\delta_z) \quad (4)$$

The interaction force in the horizontal direction is expressed as creep force in the case that the wheel flange has no contact with the rail. In contract, if the wheel flange is in contact with the rail, the wheel load and horizontal pressure act on the rail, causing the rail crown to move in the horizontal direction. In this case, torsion of the rail occurs. The torsion resistance generated by the rail and the rail fastener is expressed by a spring element.

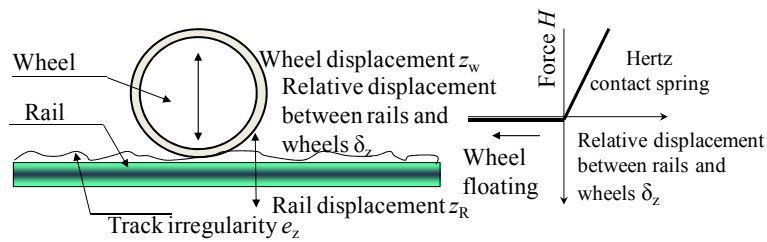


Figure 6: Wheel/ rail model.

Figure 7 shows the irregularities used for the numerical analysis. These irregularities consist of the combination of the rail irregularity and the wheel irregularity. The rail irregularity was measured on the track by a measuring device of 1m-chord versine and as for the wheel we referred to a previous research [17].

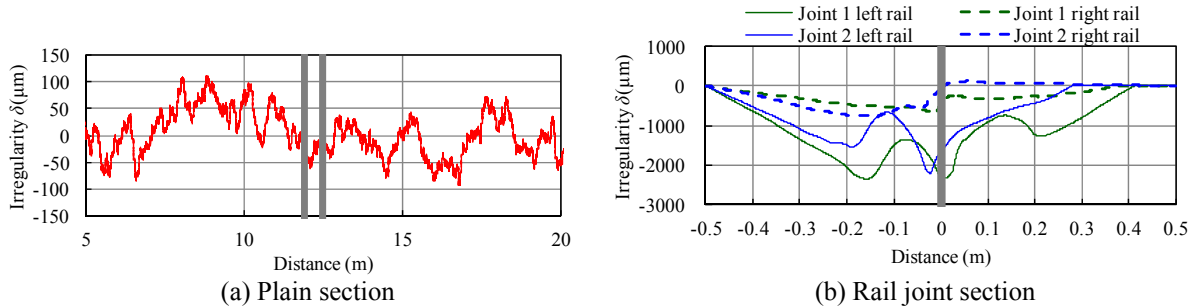


Figure 7: Irregularities used for numerical analysis.

#### (4) Solution method

In the previous paragraph, the equation of motion of the vehicle and that of the track are derived in the vehicle's coordinate system and the global coordinate system respectively. Coupling of these equations is conducted by applying the compatibility and equilibrium conditions to the sub region where both systems are connected with each other. At every moment during the train moving, the compatibility condition is evaluated using a fictitious nodal point at the center of the left and right rails where the wheelset exists.

In order to carry out efficient numerical analysis, the equations of motion concerning the vehicle and track described as equation (1) and equation (2) are transformed to modal coordinate system. The resultant equations are progressively solved in time increment  $\Delta t$  by using the *Newmark* method. However, because the equation of motion is non-linear, iterative calculation has to be carried out within  $\Delta t$  until the unbalanced force becomes sufficiently small. The mode order in the analysis is set at a value that enabled vibration up to about 2000Hz to be reproduced, and the analysis time step is set at 0.0001 sec.

#### (5) Numerical analysis condition

Table 1 shows the material dimensions and properties. Though basically the values used in the numerical analysis were derived from the Japanese design standards and the nominal values [18, 19], the spring constant of the rail pad was set at two times larger than the nominal value because of the degree of the agreement between the numerical analysis result and the measurement result of bending moment of the PC sleeper. The PC sleeper support condition was not assumed to be uniform over the whole length of the sleeper but to be nonuniform as shown in Figure 8.

Table 2 shows the numerical analysis cases. The numerical analyses were conducted with a focus on the effect of the various parameters. Basic case is underlined. The sleeper support conditions 2 and 4 were considered to be roughly corresponding to that immediate after the track maintenance. On the other hand, the sleeper support conditions 1 and 3 were considered to be corresponding to that a few days after the track maintenance.

Rail	60kg rail Young modulus $E_S = 200\text{MPa}$
Rail Pad	Spring constant $D_P = 220\text{MN/m}$ (Nominal value = $110\text{MN/m}$ )
PC sleeper	Type-6 PC sleeper PC wire = $\phi 2.9\text{mm}$ 3-strand cable 12-wires Length $L_P = 2000\text{mm}$ , Width $B_P = 240\text{mm}$ Height $H_P = 170\text{mm}$ (Rail seat), $150\text{mm}$ (Center) Concrete Young modulus $E_C = 33\text{MPa}$
	Rail joint PC sleeper PC wire = $\phi 2.9\text{mm}$ 3-strand cable 16-wires Length $L_P = 2000\text{mm}$ , Width $B_P = 300\text{mm}$ Height $H_P = 170\text{mm}$ (Rail seat), $145\text{mm}$ (Center) Concrete Young modulus $E_C = 33\text{MPa}$
Ballast	Thickness $h = 250\text{mm}$ Support spring constant $D_B = 180\text{MN/m}$ (1 rail)
Roadbed	Coefficient of subgrade reaction $K_{30} = 110\text{MN/m}^3$ Support spring constant $D_S = 111\text{MN/m}$ (1 rail) $D_T = 1/((1/D_B) + (1/D_S))$

Table 1: Material properties.

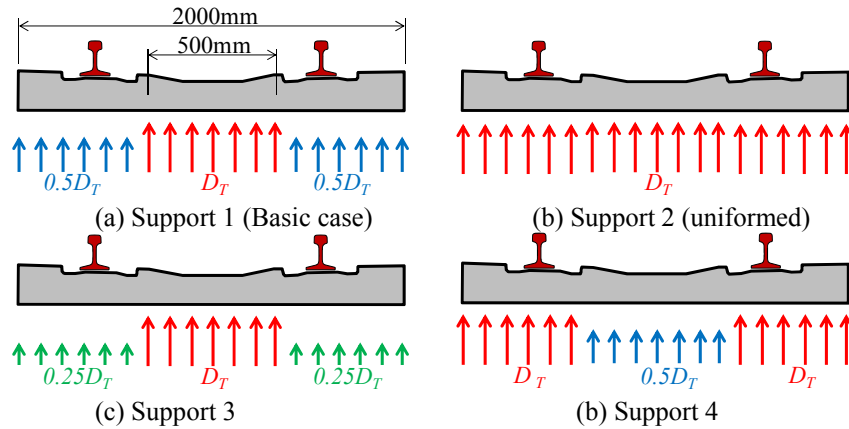


Figure 8: PC sleeper support condition.

PC sleeper	Type-6 PC sleeper, Rail joint PC sleeper
Train speed $V$	40~130km/h per 10 km/h (Basic case is <u>80km/h.</u> )
Vehicle mass $M_V$ (Passenger occupancy)	0% occupancy (= Empty) <u>50% occupancy</u> 100% occupancy
Wheelset mass $M_W$	<u><math>M_W</math></u> , $1.5M_W$ , $2.0M_W$
Irregularity	<u>Plain section</u> , <u>Joint 1</u> (see figure 7) Joint2, No-joint
Spring constant of rail pad (MN/m)	110, <u>220</u>
PC sleeper support condition	Support <u>1</u> , 2, 3, 4 (see figure 8)

Table 2: Numerical analysis cases.

### 3 INVESTIGATION RESULT

#### 3.1 Vibration mode of PC sleeper

Table 3 shows the comparison of natural frequencies of the PC sleeper vibration modes. The natural frequencies given by the numerical analyses are coincident with the measurement results excluding the rotation mode. In order to decrease this discrepancy, the accurate evaluation of the PC sleeper support condition is in need. As might be expected, the natural frequency of the rail joint PC sleeper is higher than that of the type-6 PC sleeper because the cross section and the PC wire volume of the rail joint PC sleeper are larger than that of the type-6 PC sleeper.

Mode	Type-6 PC sleeper		Rail joint PC sleeper	
	Measurement (Hz)	Numerical analysis (Hz)	Measurement (Hz)	Numerical analysis (Hz)
Vertical rigid mode	92	86	101	105
Rotation mode	102	86	74	95
1st bending mode	173	174	202	203
2nd bending mode	497	478	534	520
3rd bending mode	813	817	907	939

Table 3: Comparison of the natural frequencies of the PC sleeper vibration modes.

#### 3.2 Bending moment of the PC sleeper

Figures 9 and 10 show the comparison of the bending moments of the PC sleeper during the train running. Numerical analyses were conducted under the condition that the train speed is 80km/h and the passenger occupancy is 50%. From these figures, it can be seen that the absolute value of negative bending moments of the center of the PC sleeper are larger than that of positive bending moments of the rail seat of the PC sleeper.

Regarding the positive bending moment, the differences between “Support 1” and “Support 2” is not clear. On the other hand, regarding the negative bending moment, the bending moment of “Support 1” is almost two times larger than that of “Support 2”. In addition, the negative bending moment of “Support 1” is also coincident with the measurement result. One possible reason may be that more than one year has passed since the track maintenance, and therefore, the PC sleeper support condition has been gradually transferring from “Support 1” to “Support 2” due to the dynamic interaction between the PC sleeper and the ballast.

Figure 11 shows the relation between the train speed and the maximum bending moment of the PC sleeper during the train running. From the field measurement results, the maximum bending moment of the PC sleeper at the rail joint generated during the train running is almost 4 times larger than that in the plain section, and the maximum bending moment of the PC sleeper adjacent to the rail joint is also almost 2.7 times larger than that in the plain section. Furthermore, the bending moments of the type-6 PC sleeper are different depending on its installation section.

Regarding the comparison of the negative bending moments between “Joint 1” and “Joint 2” obtained by the numerical analyses, it can be seen that “Joint 2” is 1.5 times larger than “Joint 1”. This is due to the difference of the support condition between “Joint 1” and “Joint 2”. From the numerical analyses, it can be seen that regarding the dynamic response amplification ratio from 40km/h to 130km/h of the train speed, the rail joint PC sleeper is larger than



type-6 PC sleeper. Concretely, the ratio of the rail joint PC sleeper is 1.4 and that of the type-6 PC sleeper is 1.2.

In figure 11, the design limit values under the allowable stress design method in cases where the design wheel load is 80kN, the impact factor is 2.0, the load dispersion coefficient is 0.5, and the allowable tensile stress is  $2.0\text{N/mm}^2$  are indicated. The actual generated bending moments are under the design value.

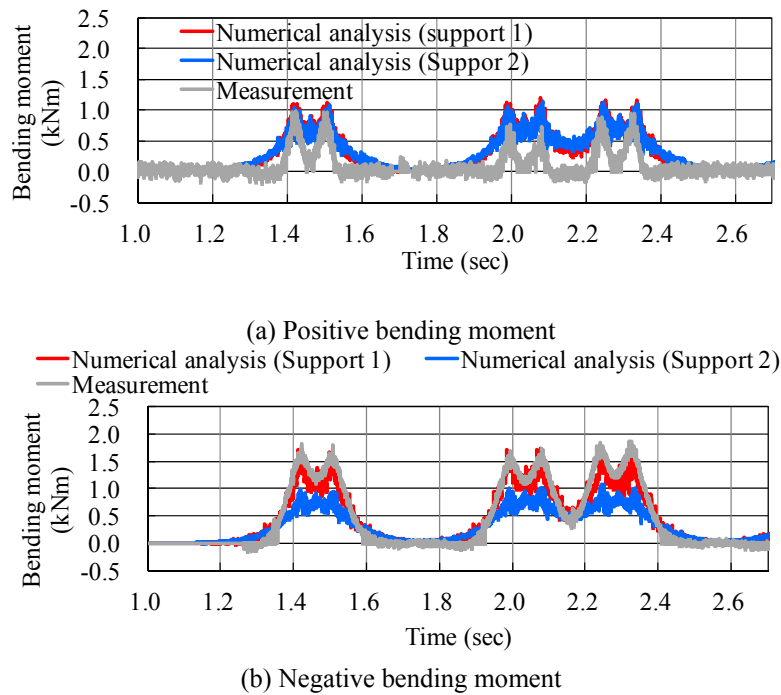


Figure 9: Comparison of the bending moment of the type-6 PC sleeper during the train running.

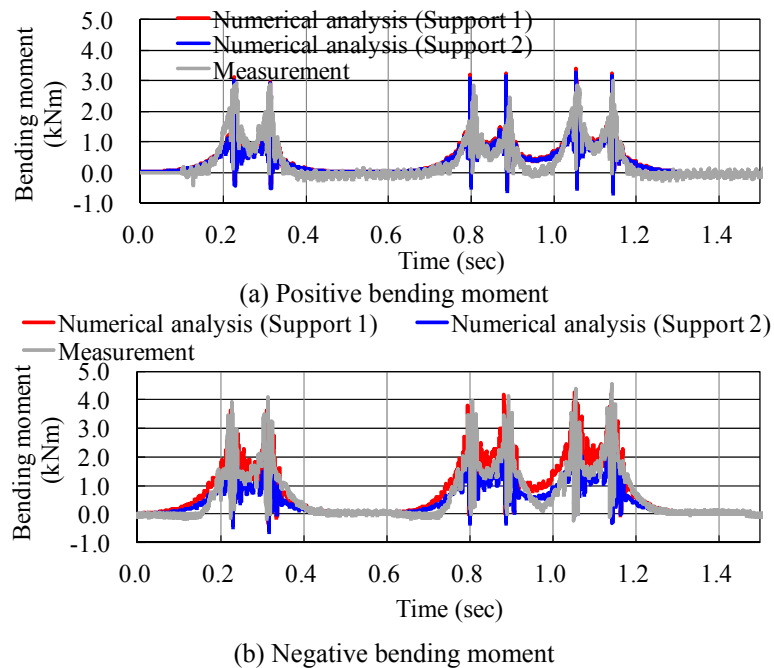
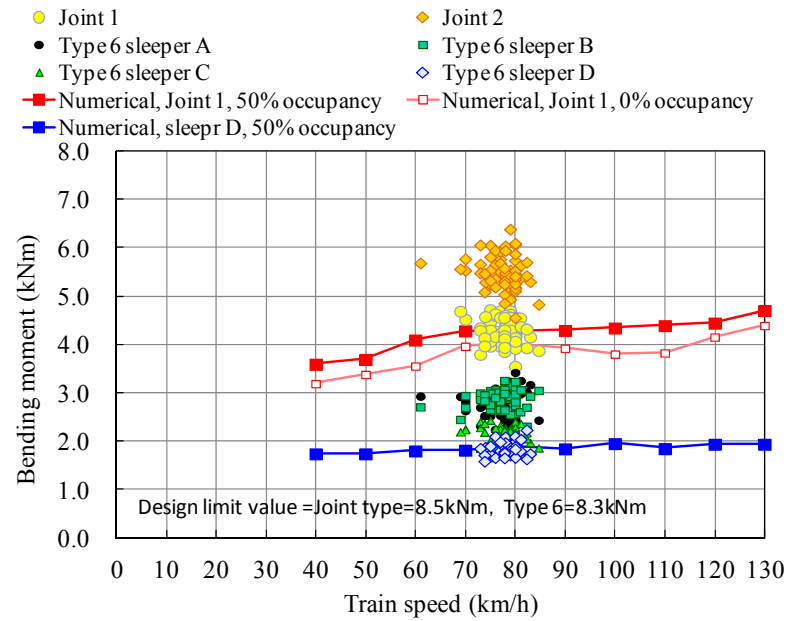
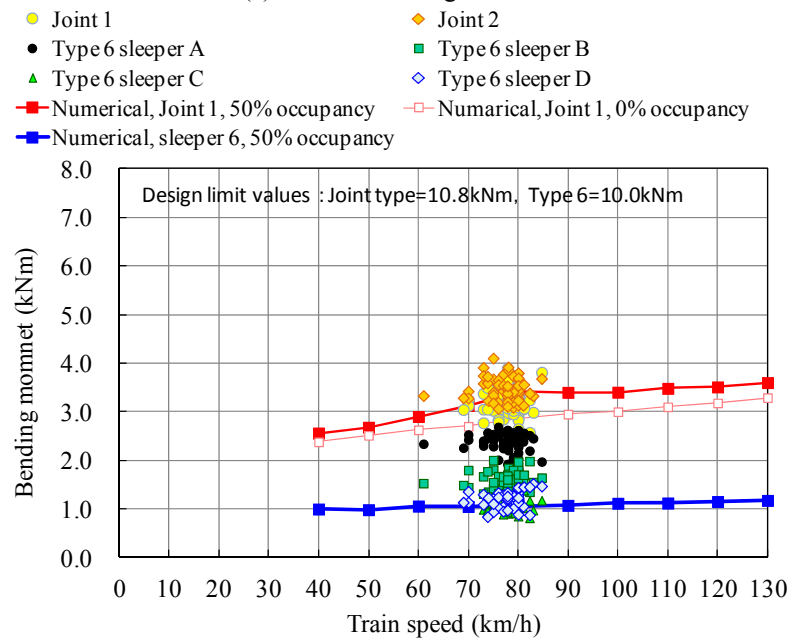


Figure 10: Comparison of the bending moment of the rail joint PC sleeper during the train running.



(a) Positive bending moment



(b) Negative bending moment

Figure 11: Relation between the train speed and the maximum bending moment of the PC sleeper during the train running.

### 3.3 Influence of various parameters

Figure 12 shows the effect of the various parameters on the bending moment of the PC sleeper during the train running. The knowledge and findings obtained by the numerical analyses in this research are shown below.

As for the passenger occupation variation, when the passenger occupation ratio increases from 50% to 100%, the bending moment increases by up to 1.2 times.

As for the wheelset mass variation, when the wheelset mass increases by 2 times, the bending moment increases by up to 1.5 times. It can be seen that negative bending moment especially is largely affected.

As for the irregularity variation, the bending moment of the PC sleeper at “Joint 1” or “Joint 2” is up to 3.4 times larger than that at “No-joint”.

Concerning the rail pad stiffness, when the spring constant of the rail pad decreases by half, the bending moment decreases by up to 20%. Furthermore, it can be seen that the bending moment in the case of “Support 3” is up to 4 times larger than that in the case of “Support 4”.

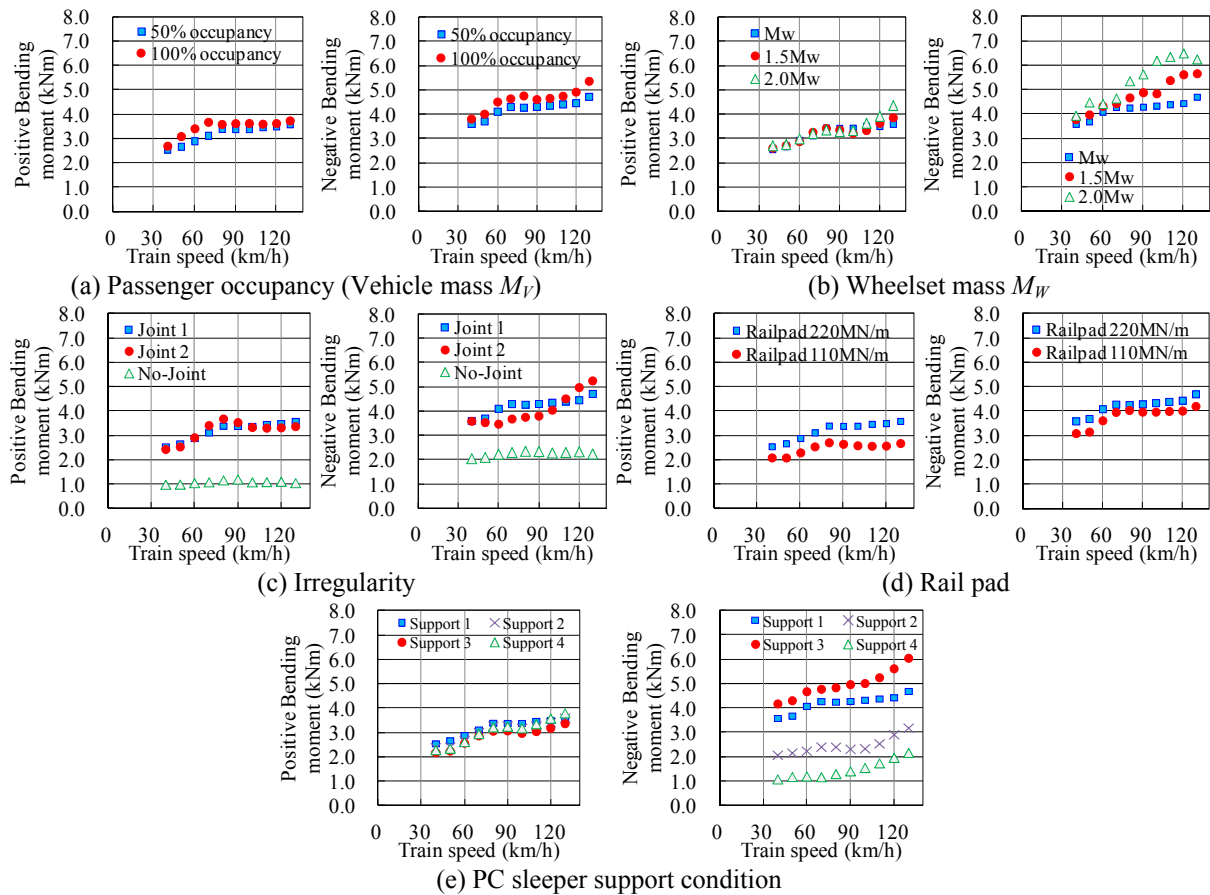


Figure 12: Effect of the various parameters on the bending moment of the PC sleeper during the train running.

### 3.4 Influence of the rail joint

Figure 13 shows the longitudinal span of the influence due to the impact wheel load at the rail joint. It can be seen that the longitudinal span of the influence is almost 4m, and there are not much difference between each case. Based on these results, the plain section, i.e. the section which is not affected by the rail joint, can be defined as a section more than a span of 4m away from the rail joint. Though length of this span absolutely depends on the given condition, this span is one of the reference values about the rail joint section. In the future, we must clarify the generality of the longitudinal span of the influence of the impact wheel load at the rail joint by increasing the sample of the irregularity and the analysis parameters.

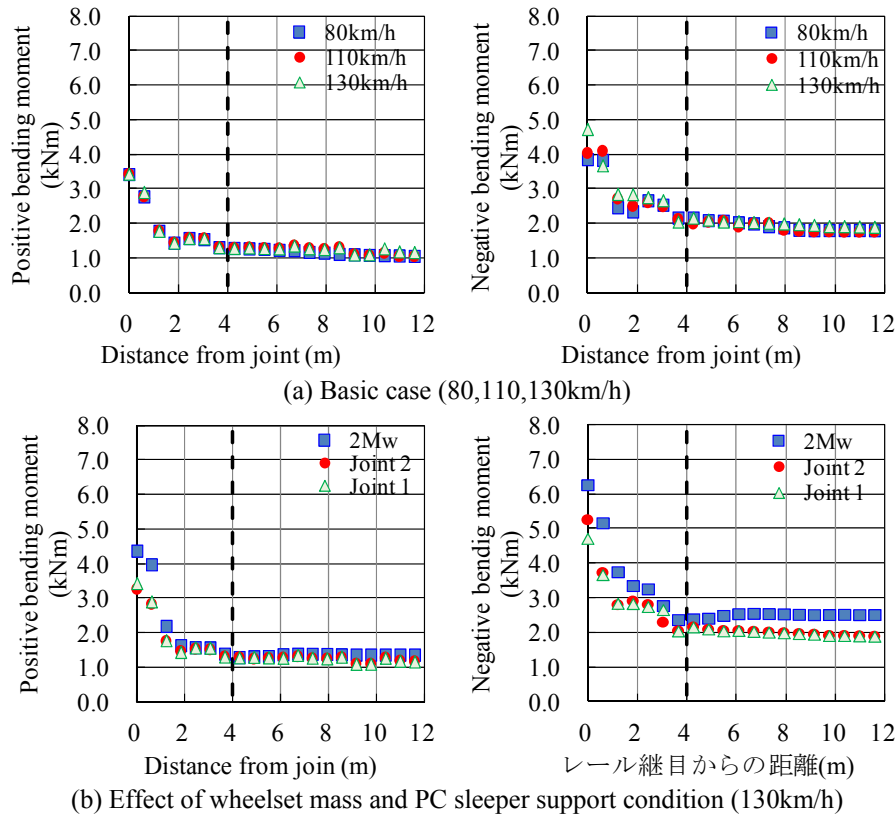


Figure 13: Longitudinal span of the influence of the impact wheel load at rail joint.

## 4 CONCRUSIONS

This research focused on the impact wheel load at the rail joints. We carried out field measurement in an operating line and numerical analyses, in order to reveal the dynamic response characteristics of the PC sleeper. The knowledge and findings obtained in this research are summarized as below.

- The field measurement results shows that the maximum bending moment of the PC sleeper at the rail joint during the train passing is almost four times larger than that in the plain section, and the maximum bending moment of the PC sleeper adjacent to the rail joint is almost 2.7 times larger than that in the plain section. Furthermore, the bending moment of type-6 PC sleeper varies depending on the measurement section.
- The absolute value of negative bending moment at the center of the PC sleeper was larger than that of the positive bending moment at the rail seat of the PC sleeper.

- Results of the numerical analyses indicate that the dynamic amplification ratio of the rail joint PC sleeper at from 40km/h to 130km/h is larger than type-6 PC sleeper. Concretely, the rail joint PC sleeper was 1.4 times, type-6 PC sleeper was 1.2 times.
- The longitudinal span of the influence of the impact wheel load at the rail joint is almost 4m.

In the future, we will reflect the concept of these knowledge and findings in the design of the PC sleeper.

## REFERENCES

- [1] H. Wakui, H. Okuda, A study on limit-state design method for prestressed concrete sleepers, *Concrete Library of JSCE*, **33**, 1-25, 1999.
- [2] H. Wakui, H. Okuda, Effects of wheel-flats on concrete sleepers, *International Symposium on precast concrete railway sleepers*, Madrid, 287-299, 1991
- [3] Joint Committee on Relation between Track and Equipment of the Mechanical and Engineering Divisions, AAR, Effect of Flat Wheels on Track and Equipment, *American Railway Engineering Association*, **53**, 1952.
- [4] ORE D 161.1 rp3, The Influence of Wheel Flats on the Track with 20 and 22.5 t Axle Loads, Utrecht, 1986.
- [5] Sakdirat Kaewunruen, Experimental and numerical studies for evaluating dynamic behavior of prestressed concrete sleepers subject to severe impact loading, *Ph.D. Thesis, Department of Civil and Mining Engineering, University of Wollongong*, 2007.
- [6] Javad Sadeghi, Investigation of Characteristics and Modelling of Railway Track System, *Ph.D. Thesis, Department of Civil and Mining Engineering, University of Wollongong*, 1997.
- [7] Zijian Zhang, Sihang Wei, Bassem Andrawes, Daniel A. Kuchma, J. Riley Edwards, Numerical and experimental study on dynamic behavior of concrete sleeper track caused by wheel flat, *International Journal of rail Transportation*, **4:1**, 1-19, 2016.
- [8] NS Vyas, AK Gupta, Modeling rail wheel-flat dynamics, *Proceedings of the 1st World Congress on Engineering Asset Management (WCEAM)*, 11-14, 2006.
- [9] J. Bian, Y.T. Gu, M. Murray, Numerical Study of Impact Forces on Railway Sleepers under Wheel Flat, *Advances in Structural Engineering*, **16:1**, 2013.
- [10] D.Kishore Kumar, K.Sambasivarao, Static and Dynamic Analysis of Railway Track Sleeper, *International Journal of Engineering Research and General Science*, **2:6**, 2014.
- [11] Masaki Sue, Yuki Okumura, Yuichiro Hori, Takayuki Onodera, Development of an Ideal Sleeper, *JR EAST Technical Review*, 29, 2015.
- [12] Kodai Matsuoka, Kiyoyuki Kaito, Hidekazu Ishii, Statistical consideration regarding the vibration characteristics and variation factors of 24-span steel railway bridge in 86 years in service, *Japan Society of Civil Engineers*, **68:3**, 157-174, 2012(In Japanese).
- [13] Tomonori NAGAYAMA, Masato ABE, Yozo FUJINO, Kenji IKEDA, Non-iterative identification of non-proportionally damped system from ambient vibration measure-

- ment and analysis of dynamic properties of a long span suspension bridge, *Japan Society of Civil Engineers*, **745**, 155-169, 2003.
- [14] H. Wakui, N. Matsumoto, M. Tanabe, A Study on Dynamic Interaction Analysis for Railway Vehicle and Structures, *QR of RTRI*, **35:2**, 96-104, 1994.
  - [15] M. Tanabe, N. Matsumoto, H. Wakui, M. Sogabe, Simulation of a Shinkansen train on the railway structure during an earthquake, *Japan Journal of Industrial and Applied Mathematics*, **28-1**, 223-236, 2011.
  - [16] M. Tanabe, S. Komiya, H. Wakui, N. Matsumoto, M. Sogabe, Simulation and visualization of high-speed Shinkansen train on the railway structure, *Japan Journal of Industrial and Applied Mathematics*, **17**, 309-320, 2000.
  - [17] Toshiki Kitagawa, Kaoru Murata, Kiyoshi Nagakura, Roughnesses on the wheel and rail surfaces for conventional narrow-gauge lines, *J-rail2007*, 515-518, 2007(In Japanese).
  - [18] Railway Technical Research Institute. Design Standards for Railway Structures and Commentary (Concrete Structures), 2007.
  - [19] Railway Technical Research Institute. Design Standards for Railway Structures and Commentary (Track structures), 2012.